






Cite this: *Sens. Diagn.*, 2022, 1, 750

## Uniformity of spheroids-on-a-chip by surface treatment of PDMS microfluidic platforms

Neda Azizipour, <sup>a</sup> Rahi Avazpour, <sup>b</sup> Mohamad Sawan, <sup>cde</sup>  
Derek H. Rosenzweig <sup>†\*fg</sup> and Abdellah Aji <sup>†\*ch</sup>

Spheroids have emerged as a reliable model in preclinical oncology research. Uniformity of spheroids is the key parameter in the reproducibility and precision of drug test results. Microfluidic-based biochips have many advantages over other spheroid formation methods, including better control over the size of spheroids. Decreasing the cell adhesion to the surface is one of the most important challenges in microfluidic platforms, which could be controlled by appropriate surface engineering methods. We have studied the effect of surface modification of PMDS microfluidic biochips with two commonly used anti-fouling coating materials, BSA and Pluronic F-68, on the uniformity of spheroids produced on-chip. The optimized PDMS surfaces effectively inhibited cell adhesion into the surfaces and promoted cell self-aggregation to produce homogenous and uniform spheroids on-chip. This work highlights the importance of surface modification on the quality and quantity of spheroid formation on microfluidic-based biochips.

Received 7th January 2022,  
Accepted 2nd May 2022

DOI: 10.1039/d2sd00004k

rsc.li/sensors

### 1. Introduction

The tumor microenvironment is known to play a crucial role in the development of cancer.<sup>1,2</sup> It is therefore important to mimic the *in vivo* like tumor microenvironment *in vitro*, to better study the mechanisms of cancer progression and enhance new therapeutics. Studies on cancer mostly rely on 2D cell culture models using immortalized cell lines.<sup>1</sup> However, it is known that signals from the extracellular matrix and 3D tumor microenvironment play a crucial role in the maintenance of tissue specifications.<sup>3</sup> Nevertheless, tumor cells respond to chemotherapy and environmental cues differently when they are cultured in a 3D

microenvironment.<sup>1,4</sup> 3D cell culture has gained much attention over the past decades with its evident advantages of more physiologically relevant data and more predictive responses in drug discovery and disease modeling.<sup>5</sup> Among various 3D cell culture models, spheroids are cell aggregations formed by self-assembly which act as excellent physiologically relevant models to provide more reliable therapeutic readouts.<sup>6,7</sup> Spheroids can be made from cancer cell lines or cells isolated from patients.<sup>8,9</sup> These *in vitro* models can reproduce some physiological aspects of *in vivo* tumors such as non-uniform distribution of nutrients and oxygen, limited availability of nutrients and/or drugs in their center, various metabolisms, and proliferation of cells in different parts of the spheroids, and being drug resistance.<sup>6</sup> They also have gene expression profiles similar to native tumors when compared with 2D models.<sup>10</sup> The size, geometry, and compactness level of spheroids directly influence the spheroid viability and drug uptake profile.<sup>11,12</sup> However, the production of uniform and homogenous spheroids is the main challenge for their broad use in cancer research.<sup>11–13</sup>

Accordingly, developing platforms to simply provide size-controlled spheroids is crucially important. Microfluidics, which is the science of working with fluids in very small quantities (between 10<sup>-9</sup> and 10<sup>-18</sup> liters) in a set of micro-channels with dimensions in the range of tens to hundreds of micrometers, has recently been employed by various research groups worldwide to generate spheroid-based tumor-on-chip models.<sup>14–16</sup> However, the quantity, and quality of spheroids formed in these platforms and the ability

<sup>a</sup> Institut de Génie Biomédical, Polytechnique Montréal, Montréal, QC H3C 3A7, Canada. E-mail: neda.azizipour@polymtl.ca

<sup>b</sup> Department of Chemical Engineering, Polytechnique Montréal, Montréal, QC H3C 3A7, Canada. E-mail: Info@recutex.ca

<sup>c</sup> Institut de Génie Biomédical, Polytechnique Montréal, Montréal, QC H3C 3A7, Canada

<sup>d</sup> Polystim Neurotech Laboratory, Electrical Engineering Department, Polytechnique Montréal, QC H3T 1J4, Canada

<sup>e</sup> CenBRAIN Laboratory, School of Engineering, Westlake University, and Westlake Institute for Advanced Study, Hangzhou 310024, China. E-mail: sawan@westlake.edu.cn

<sup>f</sup> Department of Surgery, McGill University, Montréal QC H3G 1A4, Canada. E-mail: derek.rosenzweig@mcgill.ca

<sup>g</sup> Injury, Repair and Recovery Program, Research Institute of McGill University Health Centre, Montréal, QC H3H 2R9, Canada

<sup>h</sup> NSERC-Industry Chair, CREPEC, Chemical Engineering Department, Polytechnique Montréal, Montréal, QC H3C 3A7, Canada.

E-mail: abdellah.aji@polymtl.ca

† These authors contributed equally.



to provide long-term monitoring of cellular activities are still among the remaining challenges.

Spontaneous spheroid formation occurs when cell-cell interactions dominate over cell-substrate interactions. Numerous studies have demonstrated that material surface properties (e.g. surface wettability, surface chemistry, surface charge, and roughness) influence protein adsorption on the surface, which consequently regulates cell adhesion, cellular communications, and their proliferation.<sup>17</sup> Different materials have been used to fabricate microfluidic-based cell culture devices.<sup>18,19</sup> In the past few years, polydimethylsiloxane (PDMS) has attracted much interest in microfluidic biochip fabrication due to its unique properties and particularly because of its biocompatibility, transparency, ease of fabrication, and rapid prototyping.<sup>19–21</sup> However, cell culture results on PDMS biochips greatly depend on the physicochemical properties of the PDMS surfaces.<sup>22</sup> PDMS is inherently hydrophobic due to a high surface energy barrier, which may cause challenges for the flow of aqueous solutions into the channels.<sup>1,23</sup> It is mostly believed that hydrophobic surfaces have higher levels of protein adsorption than hydrophilic surfaces.<sup>1,21,24</sup> Protein adsorption will promote cell adhesion on the PDMS surface, which consequently results in channel clogging in microfluidic-based cell culture platforms.<sup>24,25</sup> Various methods have been used by researchers to reduce cell attachment on the PDMS surfaces, yet full optimization remains to be determined.

Plasma oxygen is widely used in microfluidic devices to permanently bond PDMS layers to each other or into another surface (e.g. glass slide). Plasma oxygen introduces hydroxyl groups on the PDMS surface temporarily to render the surface hydrophilic and increase the electroosmotic flow (EOF). This leads to facilitated fluid flow into the microchannels. However, the treated PDMS surfaces can undergo hydrophobic recovery with aging time due to the migration of low-molar-mass PDMS species from the bulk to the surface.<sup>19</sup> Alternatively, surface modification with non-ionic surfactants including poly(ethylene oxide) (PEO)-terminated triblock polymers (e.g. Pluronic)<sup>26</sup> and modification with blocking molecules with strong anti-fouling properties (e.g. bovine serum albumin (BSA))<sup>27</sup> have been widely used to “block” protein adsorption and cell adhesion on the PDMS surface. PDMS chemical surface modifications to reduce protein adsorption and cell attachment have been studied earlier elsewhere.<sup>22,26,28–30</sup> However, the impact of PDMS surface modification on spheroid formation remained unclear.

Here, for the first time, the impact of PDMS surface modification on the uniformity of spheroid production on microfluidic biochip platforms has been investigated. In this work, BSA and Pluronic F-68, used as the two most common materials to treat PDMS surfaces of biochips before cell culture to decrease cell adhesion to the surface, were employed. By changing the incubation time and concentration of BSA and Pluronic F-68, various surface wettabilities and microstructures were produced on the

PDMS surface. We have observed that the surface properties of PDMS drastically affect spheroid formation on-chip. Overnight treatment of PDMS surfaces with 10% BSA provides a moderate surface wettability (around 62°) and desirable surface morphology to provide optimized surfaces with anti-fouling properties, which enhance uniform spheroid production. We believe that surface modification is an easy-to-use and cost-effective method to produce homogenous spheroids for reliable and reproducible data in drug assays and cancer research.

We anticipate that this method can lead to efficient surface treatment in microfluidic-based biochips for cancer studies.

## 2. Materials and methodology

### Fabrication of PDMS layers

Constant three-millimeter thick PDMS layers were cured by mixing the elastomer base and curing agent with a ratio of 10:1 (w/w) (Sylgard 184 Silicone elastomer kit, Dow Corning). The PDMS mixture was poured into Petri dishes. Then, they were degassed for 1 hour under vacuum to remove bubbles and cured at 65 °C in the oven for 2 h. When the PDMS samples were cured, they were cut into approximately 2.5 cm × 2.5 cm pieces.

### Surface modification of PDMS layers

The surface modification process was performed in two steps as described below.

**PDMS surface treatment with oxygen plasma.** The cured PDMS layers were exposed to oxygen plasma (liquid air, Alphagaz 1, 99.999% purity) which was set at a flow rate of 20 sccm (standard cubic centimeters) controlled by a mass flow controller (MKS 247C channel readout MKS 1259B-00100RV (0–100 sccm)). The pressure in the chamber (cylindrical with a 9” diameter and 1.25” height) was set at 600 mTorr (80 Pa) and fixed using a butterfly valve during the process. The plasma was initiated by radiofrequency plasma at 13.56 MHz (ENI model HF-300 impedance matching unit Plasma Therm AMNS 3000-E) and the applied power was set at 20 watts, with a plasma exposure time of 20 seconds per sample.

**PDMS surface treatment with chemical coatings.** To repeat each experiment in a minimum of three replicates, numerous PDMS pieces have been fabricated with soft lithography and have been treated with oxygen plasma as described above. The hydrophobic recovery of PDMS after treatment with oxygen plasma occurs due to the migration of lower molecular weight species to the surface.<sup>31</sup> Therefore, all PDMS pieces were treated with chemical coating on the 7th day after plasma exposure to provide the same physicochemical properties for all the samples before coating with chemicals. Sample surfaces were washed gently with ethanol 99% and then, samples were washed with chemical coating solutions and were immersed in their chemical coating solutions. In this study, we have chosen two different coatings with three different concentrations of each (6 different coatings in total). BSA and Pluronic F-68 which are



commonly used surface coatings to reduce cell adhesion to the surfaces have been chosen for this purpose. Chemical coatings were prepared in concentrations of 3% w/v, 5% w/v, and 10% w/v of each, to treat sample surfaces. Two time-points have been used in this study. One set of samples has been treated by immersion in freshly prepared BSA solution and Pluronic F-68 solution for approximately one hour at 37 °C, and another set of samples has been treated overnight at 37 °C to ensure maximum time for adsorption.

### Surface characterisation

**Water contact angle (WCA) measurement.** After surface treatment, each sample was gently washed with HBSS (Wisent Bioproducts, St-Bruno, QC) to remove the excess BSA and Pluronic on top of the PDMS, also to determine if the WCA changes and morphology changes on the PDMS surface were long-term or just visible due to excess Pluronic and BSA crystals on the surface. Then, the surfaces have been washed with complete cell culture media, in order to follow the same procedure which we used before the cell culture on PDMS biochips.

WCAs were measured directly on clean and flat surfaces with a goniometer (Data Physic OCA, SCA20 software) using the sessile drop technique. An intermediate equilibrium of the water–air–solid contact angle was obtained by depositing a 2 µl water droplet on the surface using a calibrated syringe. A photograph of each droplet was taken 30 s after contact with the surface by using a VCA Optima contact angle analyzer (AST products, Billerica, MA) to study the hydrophobicity. Water contact angle measurements were conducted in triplicate for each sample on the contact side.

**Atomic force microscopy (AFM) measurement.** The surface morphology of treated PDMS surfaces along with non-treated surfaces was studied using atomic force microscopy (AFM). All AFM images were captured in the air at room temperature using tapping mode on a Dimension ICON AFM (Bruker/Santa Barbara, CA). Intermittent contact imaging (*i.e.*, “tapping mode”) was performed at a scan rate of 0.8 Hz using etched silicon cantilevers (ACTA from AppNano) with a resonance frequency of around 300 kHz, a spring constant of  $\approx 42 \text{ N m}^{-1}$ , and a tip radius of 10 nm. All images were obtained with medium tip oscillation damping (20–30%).

### Fabrication of the microfluidic device to form spheroids on biochip

Each microfluidic device is composed of two PDMS layers obtained from a 3D printed master mold. The design of the channels is adapted from Astolfi *et al.*<sup>32</sup> and the parameters of each channel and wells are broadly the same as the device described by them,<sup>32</sup> except that the height of the wells has been increased to 540 µm to optimize device operation.<sup>33</sup> The bottom layer of the device consists of 2 open channels with a 600 µm wide square cross-section. Each channel is composed of five 600 µm-wide square-bottom micro-wells of 540 µm in height. The top layer PDMS with 3 mm diameter inlet and

outlet holes was bonded with plasma oxygen (the same conditions described above for PDMS surface treatment with plasma oxygen) to the bottom layer. The polymeric resin molds (HTM 140 resin, EnvisionTEC GmbH, Gladbeck, Germany) were 3D printed using a stereolithography printer (Freeform Pico and Pico 2 HD, Asiga, Alexandria, Australia).

Briefly, a mixture of PDMS (Sylgard 184 polydimethylsiloxane elastomer kit; Dow Corning, Midland, USA) base polymer and curing agent at a mass ratio of 10 : 1 was prepared and mixed well, degassed and poured into each resin mold and allowed to crosslink and cure for 2 hours in a 65 °C oven.<sup>34–37</sup> When it is cured, the PDMS layer is gently peeled off from the mold. Following surface treatment with oxygen plasma, the two layers of the PDMS were bonded together to form closed microfluidic channels and assembled into a microfluidic device.

### Surface treatment of microfluidic channels

Each microfluidic device was sterilized and air bubbles were removed from each channel by using 99.9% ethanol (Sigma-Aldrich). Then, the channels have washed a minimum of three times with chemical coating solutions (BSA or Pluronic F-68) to clean the channel surface from ethanol residues. Afterward, the channels were treated with relevant chemical coating solutions (BSA or Pluronic F-68) in order to assess the role of surface coating in reducing cell adhesion into the channels and facilitating spheroid formation on-chip. As described above, two chemical coatings have been used in this study for the surface treatment of PDMS. Triblock copolymer surfactant Pluronic F-68 (Sigma-Aldrich) and BSA (Sigma-Aldrich), which are the most commonly used materials for surface treatment in PDMS-based microfluidic devices to decrease cell adhesion to the surface, have been prepared in three different concentrations of 3% w/v, 5% w/v and 10% w/v of each to incubate with the PDMS surface. We have divided the devices into two groups to be treated with the same surface coating for two different incubation times. One group of devices has been treated with each chemical coating for approximately one hour at 37 °C, and the second group of devices has been treated overnight at 37 °C. Simply, by using P1000 micropipettes, each one of the chemical coatings has been introduced through each channel inlet and the channel was washed three to four times. Then each channel was filled with the chemical coating for the specific time designed for each group (less than one hour for group one and overnight for group two devices) and placed in the incubator (37 °C, 5% CO<sub>2</sub>, 95% ambient air).

### Cell culture and spheroid formation on-chip

MDA-MB-231-GFP cells (human mammary gland adenocarcinoma) were donated by the laboratory of Professor M. Park (McGill University) and were maintained in high glucose Dulbecco's modified eagle media (DMEM, Sigma Aldrich) supplemented with 10% (v/v) fetal bovine serum (FBS) (Sigma-Aldrich) and 1% (v/v) penicillin–streptomycin



(Sigma-Aldrich) at 37 °C, 5% CO<sub>2</sub> and 95% relative humidity (RH). Cells were seeded and passaged one or two times into 75 cm<sup>2</sup> tissue culture flasks (Corning Inc., New York, USA) before on-chip spheroid formation. 80–90% confluent cell cultures were used for the experiments on the biochip. For spheroid culture on the biochip, cells were washed with sterile phosphate-buffered saline (PBS, Sigma Aldrich) and trypsinized with 0.25% trypsin–EDTA solution (Sigma-Aldrich) to create a cell suspension right before the cell culture on the chip. Then, the microfluidic devices were removed from the incubator and the channels were rinsed three times with sterile HBSS (Wisent Bioproducts, St-Bruno, QC) to clean the channels from chemical coating residues. Then, a cell suspension with a concentration of  $5 \times 10^5$  cells per mL was introduced into the channel inlet by using a P200 micropipette. The cell suspension flowed into the channels using gravity-driven flow. The tube connected to the outlet will be lowered to approximately 10–15 cm below the inlet during the cell seeding process. Accordingly, gravity resulting from this difference in height will create a force to facilitate cell seeding. When the channels were completely filled with the cell mixture, the flow was stopped and allowed cell sedimentation into the wells. The devices were then incubated under static conditions in a humidified incubator with 5% CO<sub>2</sub> at 37 °C for 24 hours. Spheroid formation occurred by on-chip sedimentation and containment.<sup>14,15</sup> During the cell loading process into the inlet of the channels, a portion of the cells was trapped and settled down into the wells and the rest flowed into the rest of the downstream wells or were ejected through the outlet. Since the surface of the channels was treated and became cell-resistant, cell self-aggregation to form spheroids occurred inside each well within one day after the cell seeding process. On the first day post-seeding, non-adherent cells were washed off by gently rinsing the channels with complete media and cell aggregated spheroids remained inside the wells. The inlets and outlets of the devices were filled with complete media and the devices were kept in the incubator under static conditions for a period of 7 days for daily monitoring and media exchange by using P200 micropipettes.

### On-chip observation of spheroid formation and proliferation tracking

Spheroid formation and growth were imaged directly through the thin PDMS layer by using an epifluorescence inverted microscope (Axio Observer.Z1, Zeiss, Oberkochen, Germany) and sCMOS camera (LaVision, Göttingen, Germany) with the objective lens EC Plan-Neofluar 5x/0.15 for a duration of 7 days of incubation. The size of the spheroids was determined by measuring their diameters after they were imaged by fluorescence microscopy.

### ImageJ and data analysis

As explained above, spheroid images were recorded by using an epifluorescence inverted microscope (Axio Observer.Z1,

Zeiss, Oberkochen, Germany) and an sCMOS camera (LaVision, Göttingen, Germany) with the objective lens EC Plan-Neofluar 5x/0.15. To analyze the fluorescence images of the spheroids, ImageJ (National Institute of Health, Maryland, USA) was used. The fluorescence intensity of green fluorescence has been obtained with a digit value from zero to a maximum 255 with ImageJ. The analysis area of the spheroid cell culture has been carefully selected on their 2D fluorescence image. All images had a high resolution of more than 1900 dpi. The average mean diameter was calculated as  $D_m = (D_{max} + D_{min})/2$ .<sup>38</sup>  $D_m$ ,  $D_{max}$ , and  $D_{min}$  represent the mean diameter, maximum diameter, and minimum diameter of the spheroid, respectively. The average spheroid size for each type of surface treatment on days 1, 3, and 7 after cell seeding was reported as the average mean diameter for 10 spheroids per each condition  $\pm$  standard error (SE). The circularity of the spheroids has been calculated as circularity =  $D_{min}/D_{max} \times 100$ .  $D_{min}$  and  $D_{max}$  represent the minimum diameter and maximum diameter around a single spheroid, respectively (Fig. 8). The circularity of the spheroids for each type of surface treatment on days 1, 3, and 7 after cell seeding was reported as the average circularity for 10 spheroids per each condition  $\pm$  standard error (SE). The brightness level ratio (BLR) is calculated as BLR = brightness level/255  $\times$  100. By using ImageJ, the fluorescent signals obtained from the fluorescence images of the spheroids as a function of cell density in the spheroids were used as the brightness level for BLR calculations. All data have been reported as the mean  $\pm$  standard error (SE) of minimum of three independent replicates. All error bars in the figures indicate SE. Experiments were repeated at least three times per condition. One representative image is presented where the same trends were observed in multiple trials.

## 3. Results and discussion

Previous studies have demonstrated that surface treatments with BSA and poly(ethylene oxide)–poly(propylene oxide)–poly(ethylene oxide) (PEO/PPO/PEO) co-polymers (Pluronic) strongly have anti-fouling characteristics.<sup>39,40</sup> Liu *et al.*<sup>39</sup> demonstrated that PEO/PPO/PEO copolymers can modify the surface to completely prevent cell attachment. But in the present study, we have observed that the success in the surface treatment highly depends on the concentration of the chemical coating and its incubation time with the surface. The objective of this work was to study the impact of PDMS surface modification on spheroid formation on-chip. To reach this objective, we have modified the PDMS surfaces with the two popular and commonly used materials with anti-fouling properties to decrease or inhibit cell adhesion into the PDMS surfaces of microfluidic biochips. We have assessed the surface wettability and surface morphology of PDMS on treated surfaces compared with bare PDMS surfaces. Afterward, spheroid formation in various surface-treated biochips was compared in terms of the spheroid size, spherical form, and compactness level of the spheroids measured or estimated to assess the impact of surface properties on spheroid production.



### Contact angle determination

Contact angle measurements were performed for bare and treated PDMS surfaces with BSA and Pluronic F-68 coatings. Plasma treatment is an inseparable step in microfluidic biochip fabrication to permanently bond two PDMS layers together or into another surface (e.g. glass slide) to form closed microfluidic channels.<sup>1</sup> The WCA decreases immediately after plasma treatment due to the temporary presence of polar groups (e.g. SiO<sub>2</sub>, Si-OH, and Si-CH<sub>2</sub>OH) on the PDMS surface.<sup>31,41</sup> However, PDMS surfaces undergo hydrophobic recovery with aging time due to the migration of low-molar mass PDMS species from the bulk of PDMS to the surface.<sup>31,42</sup> Usually, there is a few day/week gap between the fabrication of the biochip and their use for cell culture experiments. Therefore, the PDMS surfaces go through hydrophobic recovery after this certain time and before cell culture experiments. We have mimicked this condition to provide the exact steps, which the PDMS surfaces of microfluidic biochips go through before cell culture. Therefore, first, we have treated the PDMS surface with plasma oxygen. Then, surface treatment with chemical coatings was carried out on day 7th after plasma treatment to have integrity in all data and to provide the same conditions for PDMS pieces similar to biochip surfaces before cell culture.<sup>41</sup>

It is observed that for both surface treatments with BSA and Pluronic F-68, the WCA decreased when the incubation time and concentration of chemical coatings increased. The results showed that the WCA for BSA coated surfaces decreased to close to 60 degrees, while the WCA for Pluronic F-68 coated surfaces decreased to around 82 degrees.

We have observed that the WCA of PDMS surfaces treated with BSA and Pluronic F-68 is lower than that of the bare PDMS

surface, which means that both of these surface coating materials reduced the hydrophobicity of PDMS (Fig. 1).

Previous studies have demonstrated the effect of surface wettability on protein adsorption and consequently cell adhesion to the surfaces.<sup>43–45</sup> Here, we have observed that surface treatment of PDMS with BSA and Pluronic F-68 has changed the PDMS surface wettability. Afterward, we assessed the impact of this change on cell responses to the surface and spheroid formation on-chip.

### PDMS surface topology and AFM analysis

Surface microstructure and topology are among the key parameters that affect protein adsorption and unwanted cell adhesion to the surfaces.<sup>30,43,45</sup> In the present study, we have used AFM to assess the possible topological effects on cell adhesion to the surface. The topology and microstructure of PDMS surface before and after treatment with BSA and Pluronic F-68, as the two commonly used surface coating materials in microfluidic-based devices to reduce cell adhesion to the surfaces, were characterized. In this regard, we have studied if the surface morphology of PDMS changes by surface treatment when compared with the bare PDMS. Moreover, we have investigated if this change is repeatable and reproducible in several trials. Clear changes have been observed on surface-treated PDMS layers compared with the bare PDMS. First, we have assessed the impact of incubation time. To do this, 5% BSA and 5% Pluronic F-68 were incubated with PDMS layers in two different groups. The first group was treated in less than one hour and the second group was treated overnight with surface coating materials.

AFM images of bare PDMS surfaces and treated PDMS surfaces are shown in Fig. 2.

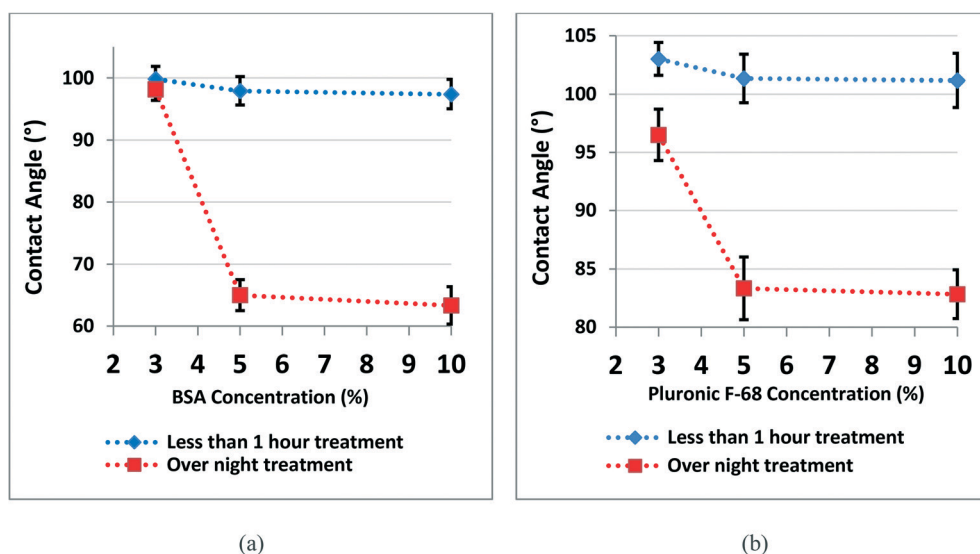


Fig. 1 Measurement of the WCA on the treated PDMS surface. a) The difference between water contact angles of PDMS coated after 1 hour and 24 hours of incubation with three concentrations of BSA; b) the difference between water contact angles of PDMS coated after 1 hour and 24 hours of incubation with three concentrations of Pluronic F-68 (error bars represent SE,  $n = 3$ ).



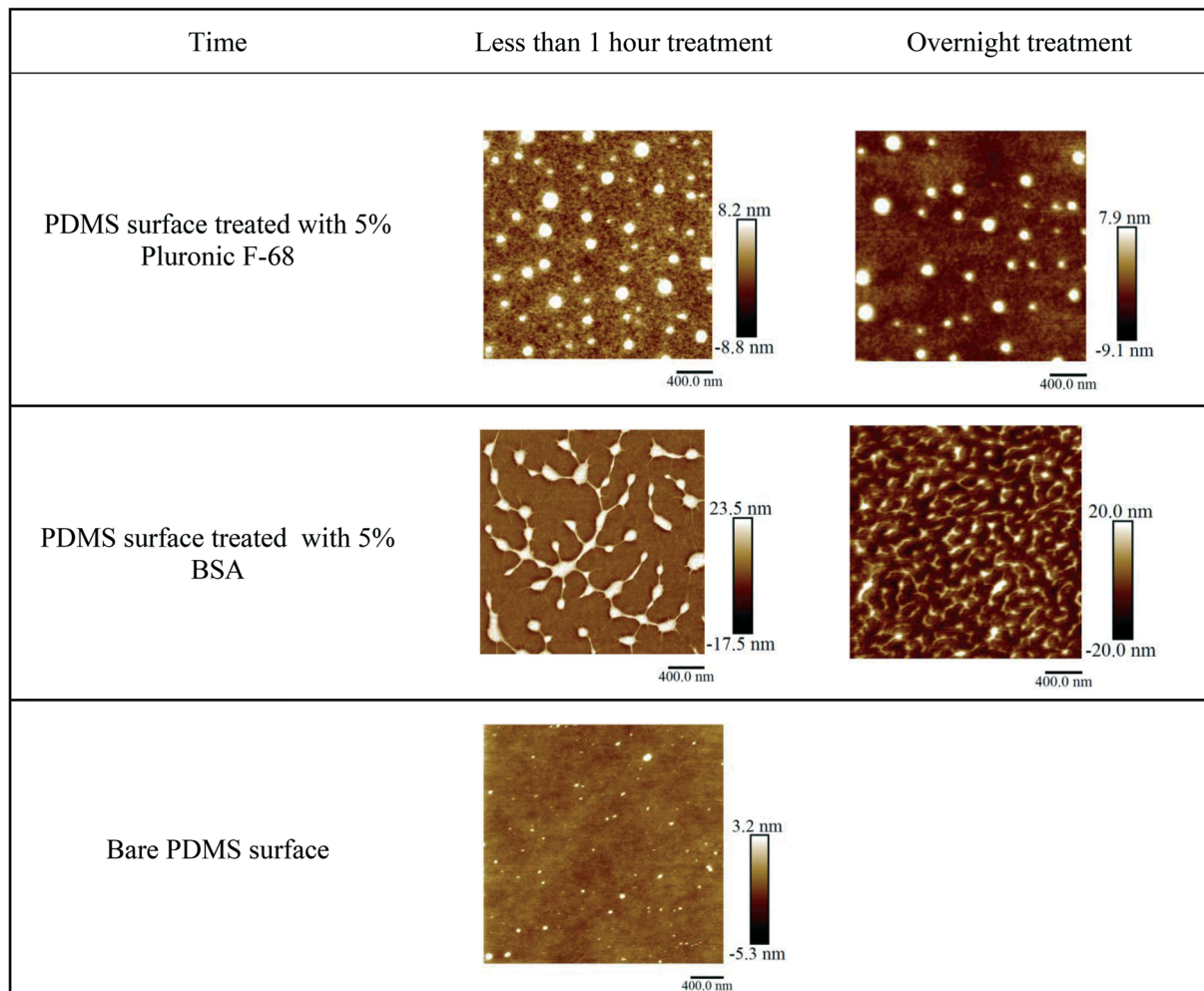


Fig. 2 AFM images of the chemical coated and bare PDMS surfaces, for less than one hour and overnight treatment with 5% BSA and 5% Pluronic F-68 vs. bare PDMS.

AFM images of treated PDMS layers have demonstrated changes in surface microstructure compared with bare PDMS. The results obtained from AFM indicate that bare PDMS surfaces have homogenous and smooth surfaces with a smaller vertical height for pick and valley structures.<sup>28,41,46</sup> Increasing the incubation time decreased the maximal vertical height for pick and valley structures. We assume that this could be related to more surface coverage by increasing the incubation time. It means that BSA or Pluronic molecules have more time to adsorb into the surfaces and cover the gaps between heights and depths on the surfaces.<sup>47</sup>

Table 1 summarizes the average maximal vertical height value for pick structures formed on PDMS surfaces after

surface treatment with BSA and Pluronic in short term (less than one hour) and long term (overnight treatment). Three AFM images were considered to calculate the average maximal vertical height of the peaks.

To assess the impact of the concentration of the coating materials, in another set of experiments, PDMS surfaces have been treated with three different concentrations of BSA and Pluronic F-68 overnight (3% w/v, 5% w/v, and 10% w/v of each). AFM images obtained from PDMS surfaces treated with different concentrations of BSA and Pluronic clearly showed the formation of peak and valley structures which proved that surface modification occurred. AFM images have demonstrated that by increasing the concentration, the

Table 1 Average maximal vertical height value for pick structures formed on PDMS surfaces after short term and long term treatment with chemical coatings (average  $\pm$  SD,  $n = 3$ )

Material	Short treatment with 5% agent	Long treatment with 5% agent
Average maximal vertical height for pick structures (nm) for surface treatment with Pluronic F-68	8.3 $\pm$ 0.8	7.9 $\pm$ 0.5
Average maximal vertical height for pick structures (nm) for surface treatment with BSA	19.1 $\pm$ 0.8	18.3 $\pm$ 0.6



maximal vertical height for pick and valley structures has been decreased. We assume that the increase in concentration provided more molecules to cover the PDMS surfaces. Therefore, more gaps and free spaces between the heights and depths on the surface have been covered. Accordingly, the height differences between height and depths on the surface decrease (Fig. 3 and Table 2).

Table 2 summarizes the average maximal vertical height value for pick structures formed on PDMS surfaces after surface treatment with different concentrations of BSA and Pluronic F-68. Three AFM images were considered to calculate the average maximal vertical height of the peaks.

As explained above and as summarized in Tables 1 and 2, Fig. 2 and 3, increasing the incubation time and concentration

of chemical coating clearly change the surface morphology of treated PDMS compared to the bare PDMS. This morphological change was repeatable and showed the formation of peaks and valley structures on the PDMS surfaces which proved that surface modification occurred and BSA and Pluronic molecules adsorbed into the PDMS surfaces.<sup>31,41,48</sup>

### Spheroid formation on microfluidic biochips

Microfluidic devices have been used in this work to assess the impact of surface modification on homogenous spheroid production, which were inspired by a design developed by Astolfi *et al.*<sup>32</sup> The design has been modified to have two separate microfluidic channels in each device. The height of

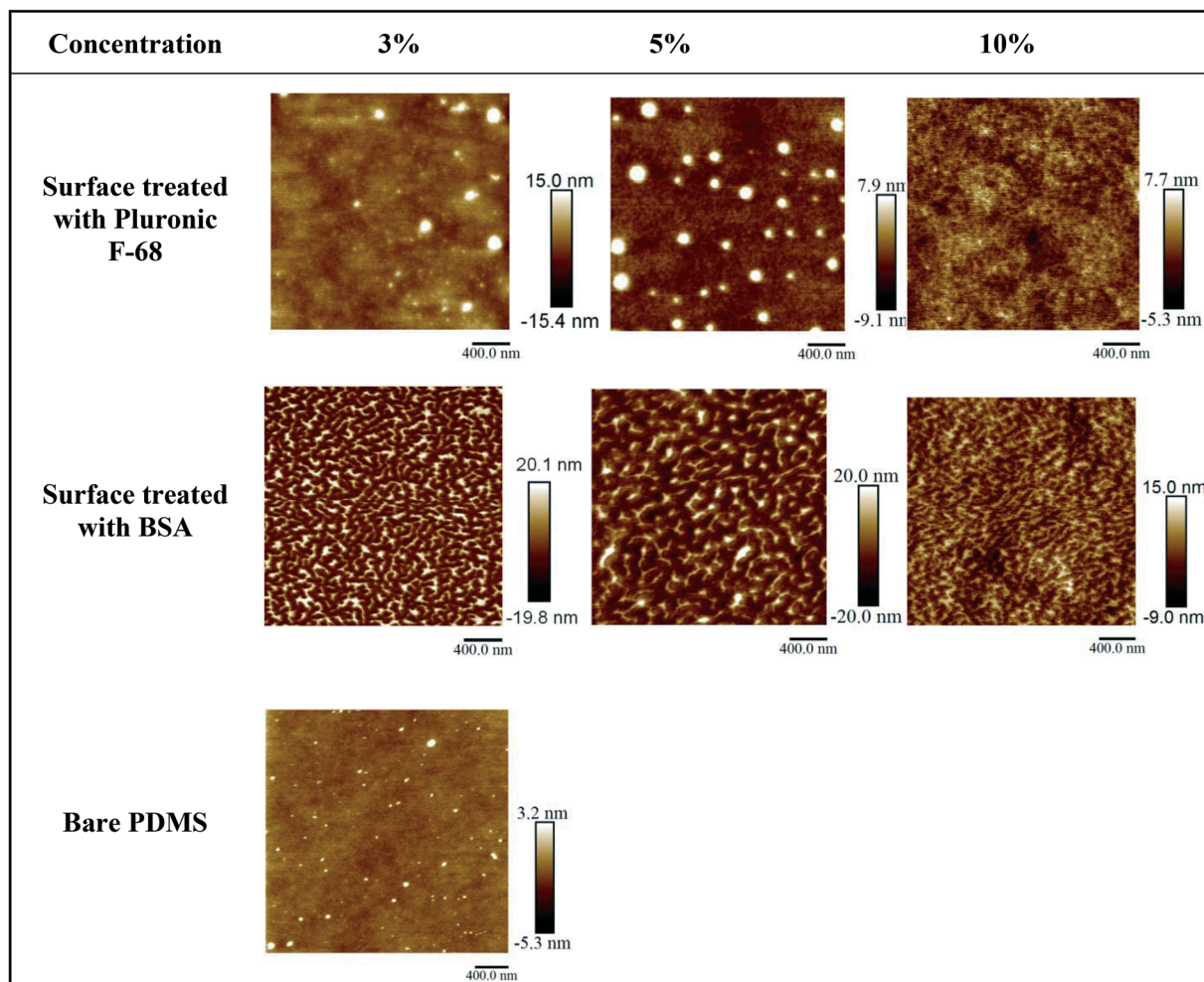


Fig. 3 AFM images of the PDMS surfaces after overnight treatment with three concentrations of chemical coatings (BSA and Pluronic F-68 vs. bare PDMS).

Table 2 Average maximal vertical height value for pick structures formed on PDMS surfaces treated with three concentrations of chemical coatings (average  $\pm$  SD,  $n = 3$ )

Material	PDMS + 3% agent	PDMS + 5% agent	PDMS + 10% agent
Average maximal vertical height for pick structures (nm) for treatment with Pluronic	13.4 $\pm$ 0.6	7.9 $\pm$ 0.5	7.8 $\pm$ 0.5
Average maximal vertical height for pick structures (nm) for treatment with BSA	25.1 $\pm$ 0.7	18.3 $\pm$ 0.6	16.8 $\pm$ 0.4
Average maximal vertical height for pick structures (nm) for bare PDMS	4.6 $\pm$ 0.4		



each well is also modified according to the theoretical simulation<sup>33</sup> for optimal cell trapping. The cell mixture of MDA-MB-231 cells is introduced into the inlet of each channel. A portion of cells was trapped and settled down into the micro-wells by sedimentation.<sup>14,15</sup> Since the surfaces were modified and became cell-repellent,<sup>25,41</sup> cell-cell adhesions became dominant over cell-substrate adhesions.<sup>11,49,50</sup> The sizes of the spheroids were relatively uniform in each group and it mostly depends on the initial cell concentration of the cell mixture. We have experimentally optimized the initial cell concentration to  $5 \times 10^5$  cells per mL in the cell mixture for our device (Fig. 4).

Microscopy observations have demonstrated that there is no significant difference between the spheroids formed in different micro-wells through the channel and have confirmed the uniform distribution of cells along the length of each channel. Fluorescence images of spheroids have shown the progressive development of spheroid sizes through 7 days of culture. Cells are capable of self-aggregating and forming cellular clusters after one day of culture and transforming into compact uniform-sized spheroids after the second day of culture. Fig. 5 demonstrates the cell aggregation process on non-treated biochips compared with devices that have been treated with chemical coatings (BSA or Pluronic F-68) to be resistant to cell adhesion into the PDMS surface. In contrast

biochips that have been treated overnight with chemical coatings, devices without any surface modifications, and devices which only have been treated for a maximum of 1 hour of incubation with chemical coating were favorable for the attachment of MDA-MB-231 cells. In these devices, cells tended to attach to the walls of the microfluidic channels and exhibited spread morphology which propagated to adherent cell clusters attached to the surfaces of the micro-wells.

The spheroid morphology on the BSA-coated and Pluronic F-68-coated devices was observed to be very similar and it seems to be mostly dependent on the concentration of the chemical coating. As a control, cells were seeded on a PDMS device without any surface treatment. A significantly greater number of cell adhesions qualitatively were observed on non-treated PMDS channels as demonstrated in Fig. 5 which illustrates the impact of surface treatment in reducing cell adhesion to the PDMS surfaces. When the PDMS surfaces of microfluidic biochips were treated with BSA or Pluronic F-68, the surfaces became cell-repellent. According to the surface characterization experiments explained above, we assume that the changes in surface wettability and microstructure of PDMS due to surface modification affected cell responses to the surface. Therefore, cell-substrate interactions decreased while cell self-agglomerations have been promoted to facilitate spheroid production. On the other hand, cells tend

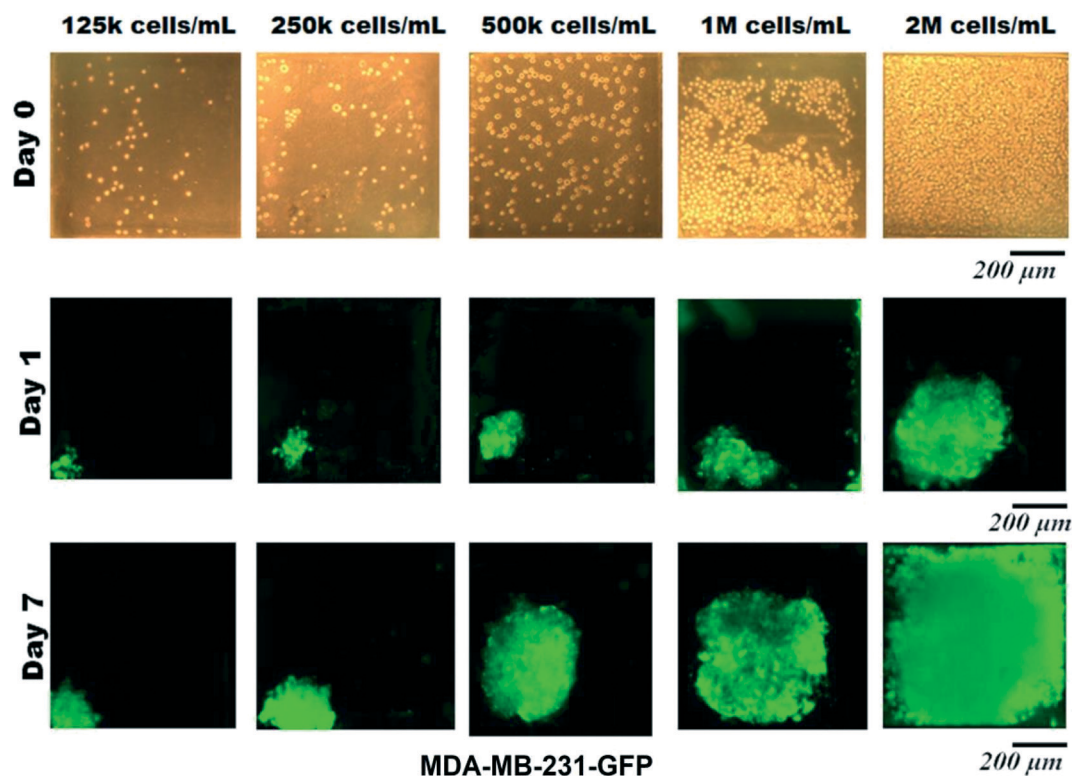


**Fig. 4** Spheroid formation on-chip with different initial cell concentrations and their growth during 7 days. Fluorescence images of MDA-MB-231-GFP spheroid formation within microchannels. Different initial cell concentrations applied to adjust the optimal initial cell concentration (size of chambers: 600, 600, 540  $\mu\text{m}$ , size of microchannel: 600  $\mu\text{m}$  width, 600  $\mu\text{m}$  height. Scale bar is 200  $\mu\text{m}$ ). The green color is due to green-fluorescent protein (GFP) in MDA-MB-231 cells. Images of the cells on day 0 (cell injection inside the microfluidic channels) were captured by bright field microscopy. Images of the spheroids on days 1 and 7 were captured by fluorescence microscopy.





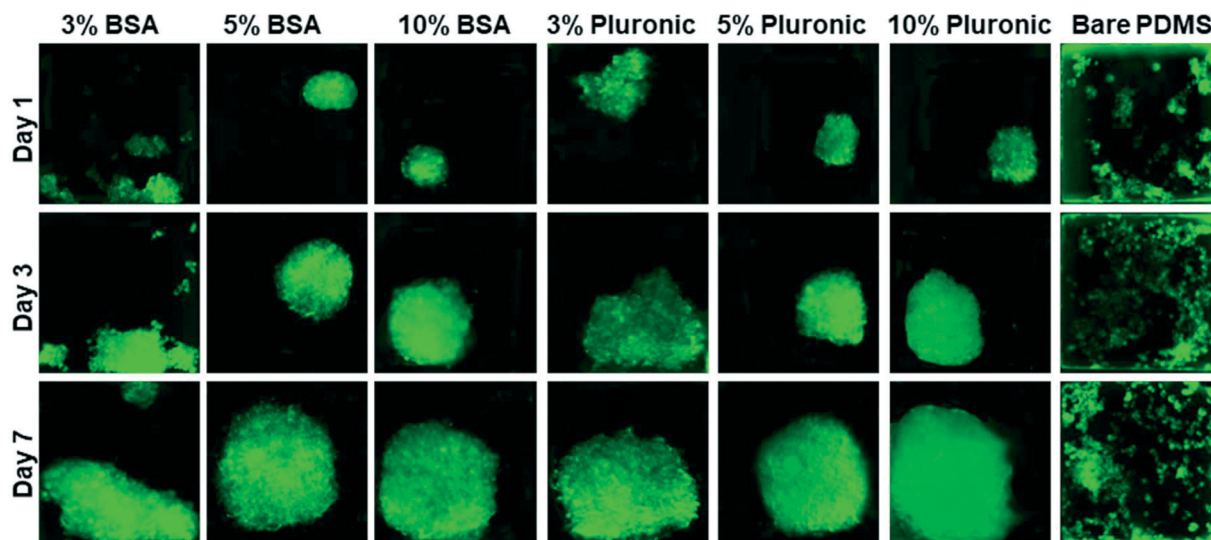


Fig. 5 MDA-MB-231-GFP spheroid formation on-chip for surfaces treated with various concentrations of chemical coatings (BSA and Pluronic F-68) compared with non-treated PDMS biochips. Each square in this image represents  $600 \mu\text{m} \times 600 \mu\text{m}$ . The green color is due to the green fluorescent protein GFP ( $n = 3$ ).

to attach to hydrophobic surfaces of non-treated PDMS biochips. Therefore, most of the micro-wells, they have proliferated randomly without the formation of spherical cell clusters. The growth pattern of the MDA-MB-231 cells within the 3D environment over the course of 1 week is shown in this figure.

### Monitoring of spheroid growth

Daily growth of spheroids has been performed by using fluorescence microscopy. In this work, we have observed that surface modification of PDMS biochips is a simple and cost-effective method to produce uniform spheroids on-chip. Our observations indicated the key role of surface modification of biochips in cell responses to the surfaces and accordingly in spheroid formation on-chip. More specifically, this work highlights the impact of incubation time and concentration of the chemical coating to modify the PDMS surface wettability and microstructure. These two were found to play a critical role in spheroid production on PDMS biochips. We need to consider that non-uniform cell aggregations, lobular structures, and loose cell-cell connections should not be considered spheroids.<sup>12,13</sup> Hence, this work highlights the crucial impact of surface modification to produce uniform and compact cell clusters, known as spheroids.

In Fig. 6 ImageJ has been used to analyze the size, spherical shape, and compactness level of spheroids during 7 days of culture. An average of 10 spheroids has been used per condition. All experiments have been repeated in three independent replicates. The brightness level of the green fluorescent color was obtained with a digit value from zero to a maximum of 255 which respectively corresponds to the darkest and brightest pixels in ImageJ. The analysis area of the spheroids has been carefully selected on the 2D fluorescence images of spheroids. The brightness level ratio

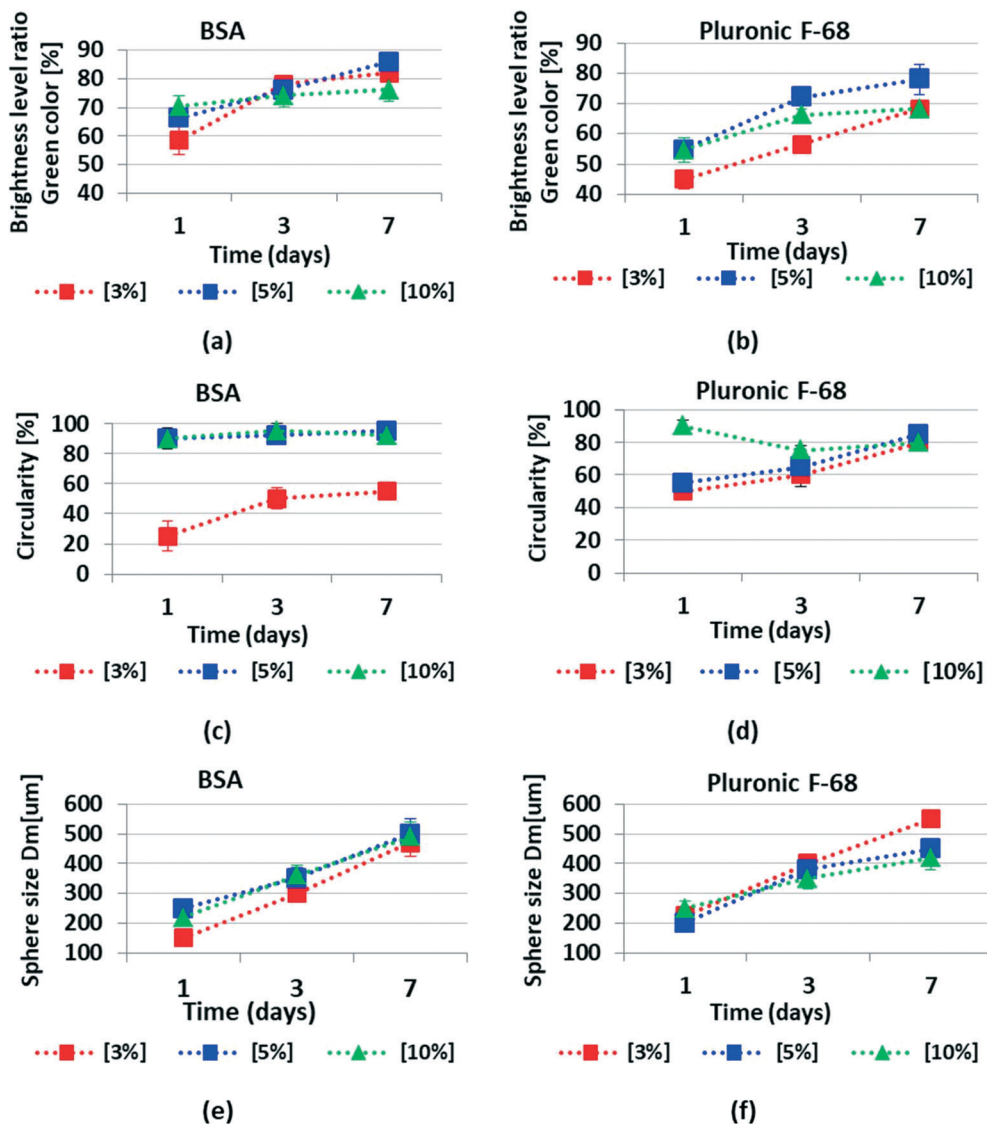
was presented as  $\text{BLR} = \text{brightness level}/255 \times 100$  in our calculations. This number qualitatively can be representative of the compactness level of spheroids. This means that when the fluorescence image is brighter, the BLR value obtained by ImageJ is a higher number. This can be representative of more cells in the spheroids that have produced more intense fluorescent signals captured by fluorescence microscopy. The BLR increased from day 1 to day 7. As explained in detail in the methodology, we have calculated the spherical shape of the spheroids as  $\text{circularity} = D_{\text{min}}/D_{\text{max}} \times 100$  around a single sphere. The spheroid size has been presented as the average mean diameter calculated as  $D_{\text{m}} = (D_{\text{max}} + D_{\text{min}})/2$ .

Fig. 6 demonstrates the changes in size, shape and compactness level of the spheroids during 7 days of culture.

Our data reveal that the BSA coating produced a cell repellent pattern similar to that observed following Pluronic F-68 surface treatment. However, BSA was more effective starting at the concentration of 5% and the optimized results have been recorded at the concentration of 10% to reduce cell adhesion to the surfaces. On the other hand, Pluronic F-68 has been shown to be effective in reducing cell adhesion to the surface starting at the concentration of 3%. According to our observations, we believe that 5% is the optimal concentration for Pluronic F-68 to achieve a higher percentage of uniformly sized spheroid formation on-chip as it seems that with 5% of Pluronic F-68, we are going to have enough surface coverage to prevent cell attachment into surfaces.

In our experiments, spheroid formation on the surface treated with 10% BSA and 5% Pluronic F-68 was greater than that to the other surfaces, suggesting that the moderate wettability (62–88 degree water contact angle) shared by these two surface coatings promoted higher cell repellent properties for PDMS surfaces.





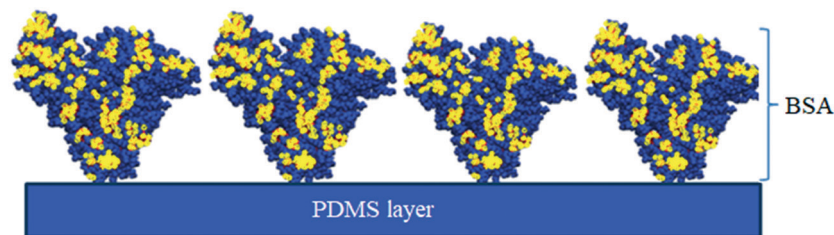
**Fig. 6** ImageJ analysis of spheroids formed in biochips treated with different concentrations of BSA and Pluronic F-68 overnight. a) and b) show the brightness level ratio of green fluorescence for BSA and Pluronic F-68 respectively. The brightness level ratio demonstrated the intensity of green fluorescence measured by ImageJ. This can be representative of the cellular concentration or compactness level of the cells inside the spheroids that produced fluorescent signals. c) and d) show the circularity of the spheroids formed in BSA and Pluronic F-68 treated biochips, respectively. Circularity can demonstrate how spheroids are spherical shaped or homogenous. e) and f) show the spheroid size measured as the average mean diameter in  $\mu\text{m}$ . 10 spheroids were used for calculations per condition. Experiments have been repeated in three independent trials (error bars represent  $\pm$  SE,  $n = 3$ ).

We believe that the concentration of the chemical coatings and the incubation time are the two important factors to regulate the surface wettability and morphology of PDMS surfaces, which provide the optimal anti-fouling property for PDMS surfaces. In this study, we only have focused on investigating the impact of PDMS surface wettability and microstructure on spheroid production on-chip. However, we need to consider that the impact of surface properties on cellular responses to the surfaces is very complicated and is not completely understood yet.<sup>22,43,51</sup> Further investigations are required for a better understanding of the influence of various surface properties on cell responses to the PDMS surfaces.

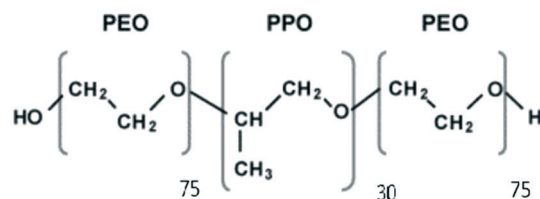
When the surface is treated with Pluronic F-68, the hydrophobic PPO head attaches to the PDMS surface while the hydrophilic PEO chains extend freely into the interface, enhancing the surface hydrophilicity and making the surface resistant to protein/cell adhesion.

Since Pluronic is much more soluble in water than in the PDMS matrix, when PDMS comes into contact with aqueous solutions of Pluronic, the hydrophilic PEO tails tend to migrate to the interface of PDMS and aqueous solution and the hydrophobic PPO heads adsorb onto the hydrophobic PDMS surface *via* physisorption and hydrophobic interaction.<sup>39,55</sup> Therefore, the hydrophobic PDMS surface will transform into a more hydrophilic and protein-resistant surface.<sup>26</sup>

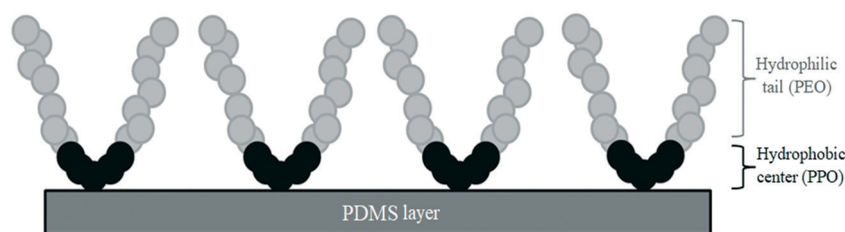




(a)



(b)



(c)

Fig. 7 (a) Schematic of BSA molecules attaching and coating the PDMS surface, (b) chemical structure of Pluronic F-68, and (c) schematic of Pluronic F-68 molecules attaching and coating the PDMS surface.

Fig. 8 shows the schematic of the 2D view of a spheroid which has been used for calculations of the average mean diameter, spheroid size, and the circularity of each spheroid. The average mean diameter is calculated as  $D_m = (D_{max} + D_{min})/2$ .<sup>38</sup> The spheroid's sizes were presented as mean diameter  $\pm$  standard deviation. The circularity of the spheroids has been reported by the circularity =  $D_{min}/D_{max}$ .

Fig. 9 demonstrates the microscopy image of the microfluidic channels and chambers, a picture of the resin mold which is fabricated by stereolithography, and a picture of the PDMS biochip which is used in this study.

Fig. 10 demonstrates the initial cell seeding process on the biochip. The cell mixture is introduced to the inlet, some of the cells will be trapped inside each well and the rest of the cells will exit through the outlet of the channel. As the inner surface of the PDMS, biochip is treated with chemical coatings and provides cell repellent properties, cells that are trapped inside the wells through sedimentation and

containment will agglomerate together and proliferate to make 3D tumor spheroids on the day after cell seeding.

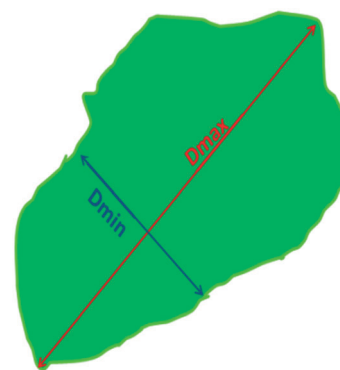


Fig. 8 Schematic of the 2D view of the spheroid and the  $D$ -maximum and  $D$ -minimum which have been used in ImageJ calculations to access the growth pattern and spheroid size over the 7 day period.



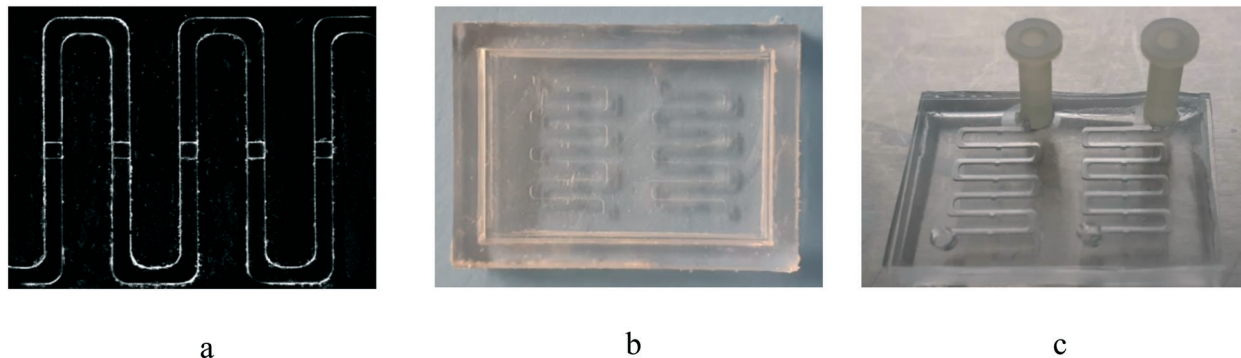


Fig. 9 Microfluidic biochip platform: (a) microscopy image of channels and chambers, (b) picture of the 3D printed resin mold, and (c) picture of the PDMS microfluidic device with inlets.

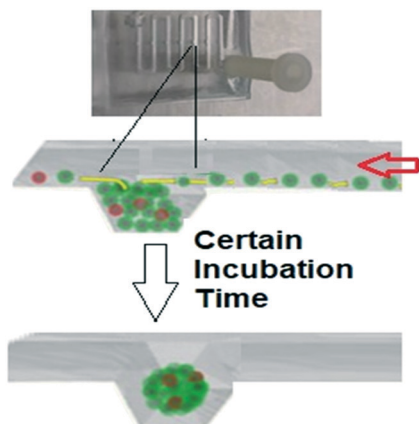


Fig. 10 Schematic illustrations of the cell seeding process and 3D spheroid formation through sedimentation and containment.

Fig. 11 shows a comparison between the different treated PDMS surfaces in terms of the number of spheroids forms on the biochip. As discussed above, between 6 studied surfaces in this work, BSA 10% shows

### Percentage of numbers of the spheroid formed in the device

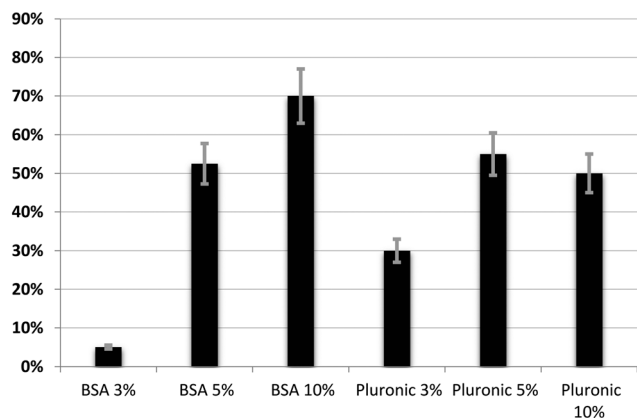


Fig. 11 Percentage of the number of spheroids formed in the device with different concentrations of chemical coatings (BSA and Pluronic F-68) (error bars represent  $\pm$  SE,  $n = 3$ ).

the best cell repellent properties by increasing the number of possible spheroids formed on the biochip. BSA 3% showed the least cell repellent properties and the lowest number of spheroids formed on-chip.

## 4. Conclusion

Understanding the correlation between surface properties and cellular responses to the surfaces is essential to designing optimal surfaces in biomedical applications including microfluidic-based biochip platforms. Although enormous studies have been performed concerning PDMS surface modifications, a systematic study on the effect of anti-fouling coating on the PDMS surface properties and its impact on spheroid production on PDMS microfluidic biochip platforms is still missing in the literature. As the cell behavior is deeply influenced by the cellular microenvironment and their substrates, the objective of this study was to investigate the influence of PDMS surface properties (specifically surface wettability and microstructure) on the uniform and homogenous spheroid production on microfluidic biochips.

In this work, we have used BSA and Pluronic F-68 as the two commonly used materials to decrease cell adhesion to the surfaces of microfluidic platforms. We have studied the effects of incubation time and concentration on changing the PDMS surface wettability and microstructure. Then, for the first time, the impacts of PDMS surface properties on spheroid formation from MDA-MB-231-GFP cells on PDMS microfluidic biochips have been investigated.

This study provides not only a fundamental understanding of the control of cell behavior in PDMS-based microfluidic platforms, but also a simple and cost-effective method to effectively enhance spheroid formation on-chip for *in vitro* assays. Our observations have demonstrated that moderately hydrophilic surfaces (62–88 degree water contact angle) promoted the highest level of cell repellent properties. Here, we have observed that overnight PDMS surface modification with 10% BSA provided an optimized surface to effectively suppress cell adhesion into the PDMS surfaces and promote spheroid formation on-chip.



In this study, we have produced homogenous and uniform-sized, and shaped spheroids in a repeatable manner. In this work, we have used breast cancer cells although the technology described here is versatile. In our future work, we will use other cell lines to assess the capability of this surface-optimized biochip to effectively capture cells from various cell lines and produce uniform spheroids on-chip. On the whole, the results of this work indicated the importance of the surface properties to modulate cell responses to the surfaces and decrease non-specific cell adhesion.

In summary, we have shown a simple, effective, practicable, and repeatable method to modify the PDMS surface of biochips to effectively enhance spheroid formation on PDMS biochips without the need to use expensive additive materials (*e.g.* hydrogel, matrigel, *etc.*) in the cell mixture to produce uniform spheroids for drug testing and cancer studies.

## List of acronyms

AFM	Atomic force microscopy
BSA	Bovine serum albumin
EOF	Electroosmotic flow
HBSS	Hank's balanced salt solution
PBS	Phosphate buffered saline
PDMS	Polydimethylsiloxane
PEO	Poly(ethylene oxide)
SD	Standard deviation
SE	Standard error
SLA	Stereolithography apparatus
3D	3 dimensions
2D	2 dimensions
WCA	Water contact angle

## Appendix

BSA is a heart shape carboxylic acid-rich protein with a molecular weight of about 66 000 Da. BSA has 584 amino acids and it contains three homologous domains which are connected by disulfide bonds.<sup>52,53</sup> BSA adsorbs on the hydrophobic surface of PMDS by the combination of hydrophobic and electrostatic interactions between BSA molecules and the PDMS surface (Fig. 7a).<sup>52,54</sup> Surface modification with BSA coating is an effective method to decrease cell adhesion to the surface due to the presence of the anti-fouling layer of BSA on the surface.<sup>47</sup>

On the other hand, Pluronic F-68 ((PEO)75-(PPO)30-(PEO)75) (Fig. 7b) with an average molecular weight of 8400 Da was chosen from the family of triblock polymers.<sup>39</sup> It has been reported that Pluronic surfactants decrease protein adsorption and cell attachment to the PMDS surface through spontaneous adsorption of their central hydrophobic poly(propylene oxide) (PPO) heads on the PDMS hydrophobic surface (Fig. 7c) which allows hydrophilic PEO tails to extend out away from the surface.<sup>26,39</sup>

## Author contributions

Conceptualization: N. A., R. A., M. S., D. H. R., and A. A.; data curation: N. A., and R. A.; formal analysis: N. A., R. A., M. S., D. H. R., and A. A.; funding acquisition: D. H. R., M. S., and A. A.; investigation: N. A., R. A., M. S., D. H. R., and A. A.; methodology: N. A., R. A., D. H. R., and A. A.; project administration: M. S., D. H. R., and A. A.; resources: M. S., D. H. R., and A. A.; supervision: M. S., D. H. R., and A. A.; validation: N. A., R. A., M. S., D. H. R., and A. A.; visualization: N. A.; writing original draft: N. A.; writing—review and editing: N. A., R. A., M. S., D. H. R., and A. A.; N. A. should be considered as the first author; D. H. R. and A. A. contributed equally to this work and should be considered as co-corresponding authors. All the authors have read and agreed to the published version of the manuscript.

## Conflicts of interest

The authors declare no conflict of interest.

## Acknowledgements

The authors gratefully acknowledge funding support from the Natural Sciences and Engineering Research Council (NSERC) of Canada discovery grants (A. A., and M. S.) and Fonds de Recherche du Quebec Sante (FRQS) Junior 2 Research Scholar Award (D. H. R.). The authors also gratefully acknowledge Professor Thomas Gervais (Polytechnique Montréal) for fruitful scientific discussions on the design and manufacturing of the biochips, and Professor Morag Park (McGill University) for kindly providing the cell line used in this study. N. A. gratefully acknowledges the scholarship from Fondation et Alumni de Polytechnique Montréal donated by the Royal Bank of Canada (RBC).

## References

- 1 S. N. Bhatia and D. E. Ingber, Microfluidic organs-on-chips, *Nat. Biotechnol.*, 2014, **32**(8), 760–772.
- 2 C. Moraes, G. Mehta, S. C. Leshner-Perez and S. Takayama, Organs-on-a-chip: a focus on compartmentalized microdevices, *Ann. Biomed. Eng.*, 2012, **40**(6), 1211–1227.
- 3 E. W. Young, Cells, tissues, and organs on chips: challenges and opportunities for the cancer tumor microenvironment, *Integr. Biol.*, 2013, **5**(9), 1096–1109.
- 4 C. Calitz, N. Pavlović, J. Rosenquist, C. Zagami, A. Samanta and F. Heindryckx, A biomimetic model for liver Cancer to study Tumor-Stroma interactions in a 3D environment with tunable Bio-Physical properties, *J. Visualized Exp.*, 2020(162), e61606.
- 5 N. Azizpour, R. Avazpour, D. H. Rosenzweig, M. Sawan and A. Ajji, Evolution of biochip technology: a review from lab-on-a-chip to organ-on-a-chip, *Micromachines*, 2020, **11**(6), 599.
- 6 X. Cui, Y. Hartanto and H. Zhang, Advances in multicellular spheroids formation, *J. R. Soc., Interface*, 2017, **14**(127), 20160877.



- 7 J. Fukuda, *et al.*, Micromolding of photocrosslinkable chitosan hydrogel for spheroid microarray and co-cultures, *Biomaterials*, 2006, **27**(30), 5259–5267.
- 8 G. Mehta, A. Y. Hsiao, M. Ingram, G. D. Luker and S. Takayama, Opportunities and challenges for use of tumor spheroids as models to test drug delivery and efficacy, *J. Controlled Release*, 2012, **164**(2), 192–204.
- 9 G. Lazzari, P. Couvreur and S. Mura, Multicellular tumor spheroids: a relevant 3D model for the in vitro preclinical investigation of polymer nanomedicines, *Polym. Chem.*, 2017, **8**(34), 4947–4969.
- 10 A. C. Luca, *et al.*, Impact of the 3D microenvironment on phenotype, gene expression, and EGFR inhibition of colorectal cancer cell lines, *PLoS One*, 2013, **8**(3), e59689.
- 11 A. S. Nunes, A. S. Barros, E. C. Costa, A. F. Moreira and I. J. Correia, 3D tumor spheroids as in vitro models to mimic in vivo human solid tumors resistance to therapeutic drugs, *Biotechnol. Bioeng.*, 2019, **116**(1), 206–226.
- 12 R. M. Sutherland, H. R. MacDonald and R. L. Howell, Multicellular spheroids: a new model target for in vitro studies of immunity to solid tumor allografts: brief communication, *J. Natl. Cancer Inst.*, 1977, **58**(6), 1849–1853.
- 13 R. M. Sutherland, W. R. Inch, J. A. McCredie and J. Kruuv, A multi-component radiation survival curve using an in vitro tumour model, *Int. J. Radiat. Biol. Relat. Stud. Phys., Chem. Med.*, 1970, **18**(5), 491–495.
- 14 A. Y. Hsiao, *et al.*, Microfluidic system for formation of PC-3 prostate cancer co-culture spheroids, *Biomaterials*, 2009, **30**(16), 3020–3027.
- 15 Y.-C. Chen, X. Lou, Z. Zhang, P. Ingram and E. Yoon, High-throughput cancer cell sphere formation for characterizing the efficacy of photo dynamic therapy in 3D cell cultures, *Sci. Rep.*, 2015, **5**(1), 1–12.
- 16 N. Dadgar, *et al.*, A microfluidic platform for cultivating ovarian cancer spheroids and testing their responses to chemotherapies, *Microsyst. Nanoeng.*, 2020, **6**(1), 1–12.
- 17 K. Y. Chumbimuni-Torres, *et al.*, Adsorption of proteins to thin-films of PDMS and its effect on the adhesion of human endothelial cells, *RSC Adv.*, 2011, **1**(4), 706–714.
- 18 K. Ren, J. Zhou and H. Wu, Materials for microfluidic chip fabrication, *Acc. Chem. Res.*, 2013, **46**(11), 2396–2406.
- 19 S. Ahadian, *et al.*, Organ-on-a-chip platforms: a convergence of advanced materials, cells, and microscale technologies, *Adv. Healthcare Mater.*, 2018, **7**(2), 1700506.
- 20 J. N. Lee, C. Park and G. M. Whitesides, Solvent compatibility of poly (dimethylsiloxane)-based microfluidic devices, *Anal. Chem.*, 2003, **75**(23), 6544–6554.
- 21 A. Gökaltun, Y. B. A. Kang, M. L. Yarmush, O. B. Usta and A. Asatekin, Simple surface modification of poly (dimethylsiloxane) via surface segregating smart polymers for biomicrofluidics, *Sci. Rep.*, 2019, **9**(1), 1–14.
- 22 F. Akther, S. B. Yakob, N.-T. Nguyen and H. T. Ta, Surface modification techniques for endothelial cell seeding in PDMS microfluidic devices, *Biosensors*, 2020, **10**(11), 182.
- 23 J. A. Vickers, M. M. Caulum and C. S. Henry, Generation of hydrophilic poly (dimethylsiloxane) for high-performance microchip electrophoresis, *Anal. Chem.*, 2006, **78**(21), 7446–7452.
- 24 B. Van Meer, *et al.*, Small molecule absorption by PDMS in the context of drug response bioassays, *Biochem. Biophys. Res. Commun.*, 2017, **482**(2), 323–328.
- 25 A. Gokaltun, M. L. Yarmush, A. Asatekin and O. B. Usta, Recent advances in nonbiofouling PDMS surface modification strategies applicable to microfluidic technology, *Technology*, 2017, **5**(01), 1–12.
- 26 H. Zhang and M. Chiao, Anti-fouling coatings of poly (dimethylsiloxane) devices for biological and biomedical applications, *J. Med. Biol. Eng.*, 2015, **35**(2), 143–155.
- 27 X. Zhang, L. Li and Y. Zhang, Study on the surface structure and properties of PDMS/PMMA antifouling coatings, *Phys. Procedia*, 2013, **50**, 328–336.
- 28 W. Zhang, D. S. Choi, Y. H. Nguyen, J. Chang and L. Qin, Studying cancer stem cell dynamics on PDMS surfaces for microfluidics device design, *Sci. Rep.*, 2013, **3**(1), 1–8.
- 29 Q. Tu, *et al.*, Surface modification of poly (dimethylsiloxane) and its applications in microfluidics-based biological analysis, *Rev. Anal. Chem.*, 2012, **31**(3–4), 177–192.
- 30 K. Boxshall, M. H. Wu, Z. Cui, Z. Cui, J. F. Watts and M. A. Baker, Simple surface treatments to modify protein adsorption and cell attachment properties within a poly (dimethylsiloxane) micro-bioreactor, *Surf. Interface Anal.*, 2006, **38**(4), 198–201.
- 31 D. Bodas and C. Khan-Malek, Hydrophilization and hydrophobic recovery of PDMS by oxygen plasma and chemical treatment—An SEM investigation, *Sens. Actuators, B*, 2007, **123**(1), 368–373.
- 32 M. Astolfi, *et al.*, Micro-dissected tumor tissues on chip: an ex vivo method for drug testing and personalized therapy, *Lab Chip*, 2016, **16**(2), 312–325.
- 33 N. Rousset, F. Monet and T. Gervais, Simulation-assisted design of microfluidic sample traps for optimal trapping and culture of non-adherent single cells, tissues, and spheroids, *Sci. Rep.*, 2017, **7**(1), 1–12.
- 34 M. Zhang, J. Wu, L. Wang, K. Xiao and W. Wen, A simple method for fabricating multi-layer PDMS structures for 3D microfluidic chips, *Lab Chip*, 2010, **10**(9), 1199–1203.
- 35 Z. Cai, W. Qiu, G. Shao and W. Wang, A new fabrication method for all-PDMS waveguides, *Sens. Actuators, A*, 2013, **204**, 44–47.
- 36 G. Comina, A. Suska and D. Filippini, PDMS lab-on-a-chip fabrication using 3D printed templates, *Lab Chip*, 2014, **14**(2), 424–430.
- 37 T. J. Hinton, A. Hudson, K. Pusch, A. Lee and A. W. Feinberg, 3D printing PDMS elastomer in a hydrophilic support bath via freeform reversible embedding, *ACS Biomater. Sci. Eng.*, 2016, **2**(10), 1781–1786.
- 38 J. M. Kelm, N. E. Timmins, C. J. Brown, M. Fussenegger and L. K. Nielsen, Method for generation of homogeneous multicellular tumor spheroids applicable to a wide variety of cell types, *Biotechnol. Bioeng.*, 2003, **83**(2), 173–180.
- 39 V. A. Liu, W. E. Jastromb and S. N. Bhatia, Engineering protein and cell adhesivity using PEO-



- terminated triblock polymers, *J. Biomed. Mater. Res.*, 2002, **60**(1), 126–134.
- 40 R. Fraioli, J. M. Manero Planella, F. J. Gil Mur and C. Mas-Moruno, Blocking methods to prevent non-specific adhesion of mesenchymal stem cells to titanium and evaluate the efficiency of surface functionalization: albumin vs poly (ethylene glycol) coating, Premio SIBB 2014, 2014.
- 41 D. Bodas and C. Khan-Malek, Formation of more stable hydrophilic surfaces of PDMS by plasma and chemical treatments, *Microelectron. Eng.*, 2006, **83**(4–9), 1277–1279.
- 42 M. Morra, E. Occhiello, R. Marola, F. Garbassi, P. Humphrey and D. Johnson, On the aging of oxygen plasma-treated polydimethylsiloxane surfaces, *J. Colloid Interface Sci.*, 1990, **137**(1), 11–24.
- 43 D. P. Dowling, I. S. Miller, M. Ardhaoui and W. M. Gallagher, Effect of surface wettability and topography on the adhesion of osteosarcoma cells on plasma-modified polystyrene, *J. Biomater. Appl.*, 2011, **26**(3), 327–347.
- 44 P. Van Wachem, *et al.*, Adhesion of cultured human endothelial cells onto methacrylate polymers with varying surface wettability and charge, *Biomaterials*, 1987, **8**(5), 323–328.
- 45 A. Ranella, M. Barberoglou, S. Bakogianni, C. Fotakis and E. Stratakis, Tuning cell adhesion by controlling the roughness and wettability of 3D micro/nano silicon structures, *Acta Biomater.*, 2010, **6**(7), 2711–2720.
- 46 Y.-W. Huang and V. K. Gupta, A SPR and AFM study of the effect of surface heterogeneity on adsorption of proteins, *J. Chem. Phys.*, 2004, **121**(5), 2264–2271.
- 47 W. Schrott, *et al.*, Study on surface properties of PDMS microfluidic chips treated with albumin, *Biomicrofluidics*, 2009, **3**(4), 044101.
- 48 S. Pinto, *et al.*, Poly (dimethyl siloxane) surface modification by low pressure plasma to improve its characteristics towards biomedical applications, *Colloids Surf., B*, 2010, **81**(1), 20–26.
- 49 R. Tzoneva, N. Faucheux and T. Groth, Wettability of substrata controls cell–substrate and cell–cell adhesions, *Biochim. Biophys. Acta, Gen. Subj.*, 2007, **1770**(11), 1538–1547.
- 50 J. Friedrich, C. Seidel, R. Ebner and L. A. Kunz-Schughart, Spheroid-based drug screen: considerations and practical approach, *Nat. Protoc.*, 2009, **4**(3), 309–324.
- 51 M. Ferrari, F. Cirisano and M. C. Morán, Mammalian cell behavior on hydrophobic substrates: influence of surface properties, *Colloids Interfaces*, 2019, **3**(2), 48.
- 52 T. A. Wani, A. H. Bakheit, M. Abounassif and S. Zargar, Study of interactions of an anticancer drug neratinib with bovine serum albumin: spectroscopic and molecular docking approach, *Front. Chem.*, 2018, **6**, 47.
- 53 D. A. Belinskaia, *et al.*, The Universal Soldier: Enzymatic and Non-Enzymatic Antioxidant Functions of Serum Albumin, *Antioxidants*, 2020, **9**(10), 966.
- 54 D. Kim and A. E. Herr, Protein immobilization techniques for microfluidic assays, *Biomicrofluidics*, 2013, **7**(4), 041501.
- 55 W. Liu, K. Han, M. Sun and J. Wang, Enhancement and control of neuron adhesion on polydimethylsiloxane for cell microengineering using a functionalized triblock polymer, *Lab Chip*, 2019, **19**(19), 3162–3167.

